IMAGE RESTORATION WITH ANTI-REFLECTIVE BOUNDARY CONDITIONS AND RE-BLURRING

Marco Donatelli[†] Claudio Estatico[‡] Stefano Serra-Capizzano[†]

[†]Università dell'Insubria - Dipartimento di Fisica e Matematica, Via Valleggio 11, 22100 Como, Italy (marco.donatelli@uninsubria.it, stefano.serrac@uninsubria.it).

[‡]Dipartimento di Matematica, Università di Genova, Via Dodecaneso 35, 16146 Genova, Italy (estatico@dima.unige.it).

AMS Subject Classification: 65F10, 65F15, 65Y20

Section 16. Numerical Analysis and Scientific Computing – Poster number: 306

Abstract

We consider the classical de-blurring problem of noisy and blurred signals or images in the case of a space invariant point spread function (PSF) with suitable boundary conditions (BCs). Our focus is on the anti-reflective BCs since they reduce substantially artifacts called ringing effects with respect to other classical choices, while preserving the same computational cost.

The Boundary Conditions

Basically, the mathematical model of image blurring with spatial invariant kernel is the following Fredholm operator of first kind

$$g(x,y) \;=\; \int_{\mathbb{R}^2} \mathcal{K}(x-\theta, y-\xi)\, f_o(\theta,\xi)\, d\theta d\xi \;+\; \nu(x,y),$$

where f_o is the (true) input object, $\mathcal{K}$ is the integral kernel of the operator, also called point spread function, ν is the noise, and g is the observed image.

In the discrete case the observed image is $n \times n$ (for simplicity we assume square images) and the PSF is $p \times p$. The corresponding matrix equation is $\mathbf{g} = K\mathbf{f}_o + \boldsymbol{\nu}$ which is under-determined since the matrix K has size $n^2 \times m^2$ with $m = n + p - 1$. An attractive technique, both from the quality of the restored images and computational point of view, is the use of appropriate *boundary conditions*: linear or affine relations between the unknowns outside the field of view (FOV) and the unknowns inside the FOV.

The most common types of BCs and related properties are summarized in the following table for the *1D case*:

Type	Description outside the FOV	Matrix structure	Matrix-vector product	Ref.
Zero Dirichlet	zero pad	Toeplitz	$O(m \log m)$ complex op.	[1]
Periodic	circular repetition	Circulant	$O(n \log n)$ complex op.	[1]
Reflective	reflection using even symmetry	Toeplitz + Hankel	symmetric PSF: $O(n \log n)$ real op. generic: $O(m \log m)$ complex op.	[2]
Anti-reflective	reflection using odd symmetry	Toeplitz + Hankel + rank 2	symmetric PSF: $O(n \log n)$ real op. generic: $O(m \log m)$ complex op.	[5]

Table 1. Features of the Boundary Conditions in the 1D case

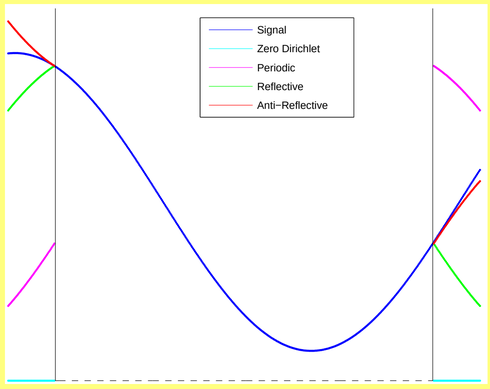

Figure 1. A signal with BCs

The generalization to the d-dimensional case can be done resorting to tensor product arguments. The computational cost is related to the algebraic actual size of the involved objects (for instance we have $O(n^d \log n)$ for the periodic BCs, if the d-dimensional object is $\underbrace{n \times n \times \cdots \times n}_{d}$) .

The Antireflective BCs (AR-BCs)

For the sake of simplicity we explain the imposition of AR-BCs in the 1D case. We emphasize that in the 2D there is not a unique choice at the vertices of the image (see [3]).

Let $\mathbf{f}_0 = (\ldots, f_0, f_1, \ldots, f_n, f_{n+1}, \ldots)^T$ and $\mathbf{h} = (\ldots, 0, 0, h_{-p}, h_{-p+1}, \ldots, h_0, \ldots, h_{p-1}, h_p, 0, 0, \ldots)^T$, with $\sum_{j=-p}^{p} h_j = 1$, be the original signal and the blurring functions. We set

$$f_{1-j} = f_1 - (f_{j+1} - f_1) = 2f_1 - f_{j+1}, \qquad f_{n+j} = f_n - (f_{n-j} - f_n) = 2f_n - f_{n-j},$$

for $j = 1, \ldots, p$. Then $K\mathbf{f}_o = \mathbf{g}$ becomes $A\mathbf{f} = \mathbf{g}$, with $A \in \mathbf{R}^{n\times n}$. The matrix A is a Toeplitz+Hankel plus a 2 rank correction matrix, where the correction is placed at the first and the last columns. Furthermore, in the case of symmetric PSF, A belongs to a matrix algebra denoted by S_1, such that the matrix vector product with A, the solution of a the linear system $A\mathbf{f} = \mathbf{g}$, and the eigenvalues of A can be computed in $O(n \log(n))$ operations, basically using the discrete fast sine transforms (DST-Is). The matrix algebra S_1 can be introduced as follows (see [4]). Let $Q = Q_n$ be the n-by-n orthogonal and symmetric matrix expressed by $[Q]_{i,j} = \sqrt{\frac{2}{n+1}} \sin\left(\frac{ji\pi}{n+1}\right)$, $i, j = 1, \ldots, n$, then we define $\tau_n = \{QDQ : D \text{ is a real diagonal matrix of size } n\}$. Now, by definition, $M \in \mathcal{S}_1$ if

$$M = \begin{bmatrix} \alpha & & \\ \mathbf{v} & \hat{M} & \mathbf{w} \\ & & \beta \end{bmatrix},$$

with $\alpha, \beta \in \mathbf{R}$, $\mathbf{v}, \mathbf{w} \in \mathbf{R}^{n-2}$ and $\hat{M} \in \tau_{n-2}$. Furthermore, any anti-reflective matrix is related to a particular generating function so that the basic arithmetic operations between anti-reflective matrices can be resorted to simple function operations. In addition, anti-reflective matrices are diagonalized by a "quasi-orthogonal" transform.

The previous considerations can be generalized to the d-dimensional case obtaining the S_d algebra.

The normal equations and the re-blurring

Regularization methods extensively used in the literature (e.g., Tikhonov regularization, CGNE, Landweber) are generally applied to the normal equations $A^TA\mathbf{f} = A^T\mathbf{g}$, where $A \in \mathbf{R}^{n^2\times n^2}$ in the image deblurring. For the first two kinds of BCs of Table 1 and in the case of reflective BCs (R-BCs) and centrosymmetric PSF, the algebraic transposition of the coefficient matrix is equivalent to a 180° rotation of the PSF. Unfortunately, this statement is wrong for AR-BCs. Thus when the AR-BCs are applied to the normal equations, they lose the good computational properties described in the previous section, since the algebra S 1 is not closed under transposition. As a consequence, in some cases AR-BCs lose their supremacy in the restoration with respect to the other BCs. Therefore, instead of dealing with normal equations, we always work with $A'A\mathbf{f} = A'\mathbf{g}$ where A' is the matrix obtained imposing the current BCs to the 180° rotated PSF (in the general d-dimensional case, the PSF is flipped along each of the d directions). We emphasize that the classical normal equations and our approach are different only in the AR-BCs case and in the case of R-BCs and noncentrosymmetric PSF. With this new formulation, the AR-BCs become again computationally equivalent to the R-BCs and are the better choice regarding the quality of the restored image. This technique is known as *re-blurring* (see [4]). In particular, from a computational point of view, we have that $A'A \in S_2$ since $A' \in S_2$, while, in general, $A^TA \notin S_2$. This allows us to keep the $O(n^2 \log(n))$ computational cost for the solution of the linear system in the case of strongly symmetric PSFs.

Numerical experiments

We test the BCs deblurring techniques for the following two problems. The first one, in Figure 2, has a Gaussian function that is strongly symmetric and Gaussian noise. The second one, in Figure 3, is an astronomical setting with a nonsymmetric PSF and Poissonian noise. The FOV in the true images is denoted by a white square.

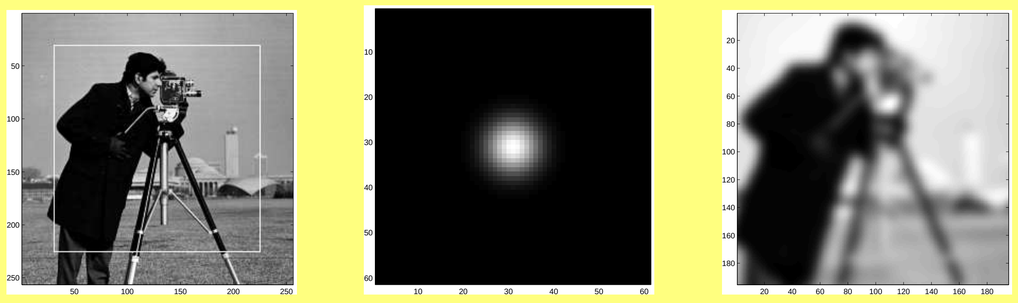

True image Gaussian PSF Blurred image

Figure 2. Test I: cameramen with Gaussian PSF

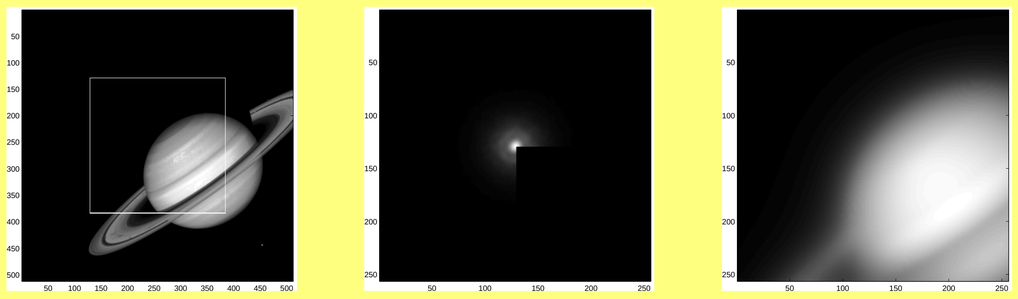

True image Experimental PSF Blurred image

Figure 3. Test II: Saturno with astronomical PSF

Table 2 shows the best relative restoration errors (RREs) among the first 200 iterations of the CG method for different levels of noise. The signal to noise ratio (SNR) is defined as $20 \log_{10} ||\mathbf{g}_b||_2/||\nu||_2$, where $\mathbf{g}_b$ is the blurred image without noise and ν is the noise vector (SNR $= \infty$ means 0% of noise). Although some positive effects arise in all cases, the choice of the anti-reflective BCs is important mainly if the noise on the data is low (i.e., for high values of SNR) and when the PSFs has a large support (like for instance in Test II). Figure 4 shows the three optimal deblurred images, for different BCs.

	Test I (Figure 2)			Test II (Figure 3)		
SNR	**Periodic**	**Reflective**	**Anti-Reflective**	**Periodic**	**Reflective**	**Anti-Reflective**
∞	0.2275	0.1993	0.1831	0.2353	0.1521	0.0816
50	0.2276	0.1996	0.1850	0.2353	0.1521	0.0819
40	0.2278	0.2007	0.1921	0.2356	0.1525	0.0837
30	0.2300	0.2088	0.2051	0.2371	0.1552	0.1063
20	0.2487	0.2382	0.2378	0.2529	0.1807	0.1553

Table 2. Best relative restoration errors within 200 iterations of CG method applied to $A'A\mathbf{f} = A'\mathbf{g}$.

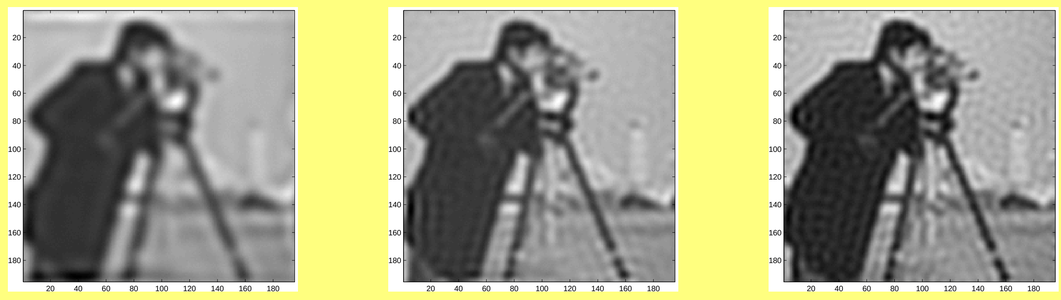

Periodic Reflective Anti-Reflective

Figure 5. Best restorations for the Test I

Graphs of convergence histories are plotted in Figure 5. They show the RREs vs. the iteration number for the Test I and two different levels of noise. In any case, the Anti-Reflective BCs provide the best results and the corresponding curves are quite flat. In this way, the estimation of the stop iteration, which generally is a difficult task, is simpler with AR BCs.

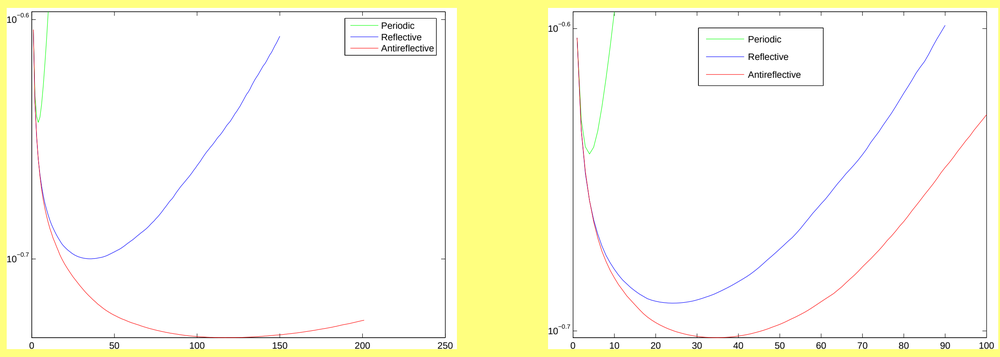

SNR = 50 SNR = 35

Figure 5. Relative restoration errors vs iteration number for the Test I

References

[1] M. Bertero and P. Boccacci 1998, *Introduction to inverse problems in imaging*, Inst. of Physics Publ. Bristol and Philadelphia, London, UK.

[2] M. Ng, R. H. Chan, and W. C. Tang 1999, A fast algorithm for deblurring models with Neumann boundary conditions, *SIAM J. Sci. Comput.*, 21, pp. 851–866.

[3] M. Donatelli, C. Estatico, J. Nagy, L. Perrone and S. Serra-Capizzano, Anti-reflective boundary conditions and fast 2D deblurring models, *SPIE's 48th Annual Meeting*, August 2003 in San Diego, CA USA, F. Luk Ed, Vol. 5205 pp. 380-389.

[4] M. Donatelli and S. Serra Capizzano 2005, Anti-reflective boundary conditions and re-blurring, *Inverse Problems*, 21 pp. 169–182.

[5] S. Serra Capizzano 2003, A note on anti-reflective boundary conditions and fast deblurring models, *SIAM J. Sci. Comput.*, 25, pp. 1307–1325.